Dispersion of Single-Walled Carbon Nanotubes in Aqueous Solutions of the Anionic Surfactant NaDDBS

Olga Matarredona,[†] Heather Rhoads,[‡] Zhongrui Li,[†] Jeffrey H. Harwell,[†] Leandro Balzano,[‡] and Daniel E. Resasco*[,†]

School of Chemical Engineering and Materials Science, University of Oklahoma, Norman, Oklahoma 73019, and SouthWest Nanotechnologies Inc., Norman, Oklahoma 73069

Received: August 22, 2003; In Final Form: October 2, 2003

The insolubility of single-walled carbon nanotubes (SWNT) in either water or organic solvents has been a limitation for the practical application of this unique material. Recent studies have demonstrated that the suspendability of SWNT can be greatly enhanced by employing appropriate surfactants. Although the efficiency of anionic, cationic, and nonionic surfactants has been demonstrated to different extents, the exact mechanism by which carbon nanotubes and the different surfactants interact is still uncertain. To deepen the understanding of this interfacial phenomenon, we have investigated the effects of chemical modifications of the surface on the extent of nanotube−surfactant interaction. Such changes in the surface chemistry of the SWNT can be achieved by simply varying the pretreatment method, which can be acidic or basic. We have found that intrinsic surface properties such as the PZC (point of zero charge) are greatly affected by the purification method. That is, the electrical charge of the SWNT surface varies with the pH of the surrounding media. However, it has been found that during the adsorption of the anionic surfactant sodium dodecylbenzenesulfonate (NaDDBS) on SWNT Coulombic forces do not play a central role, but are overcome by the hydrophobic interactions between the surfactant tail and the nanotube walls. Only at pH values far from the PZC do the Coulombic forces become important. The hydrophobic forces between the surfactant tail and the nanotube determine the structure of the surfactant-stabilized nanotubes. In such a structure, each nanotube is covered by a monolayer of surfactant molecules in which the heads form a compact outer surface while the tails remain in contact with the nanotube walls. It is important to note that although the final configuration can be described as a cylindrical micelle with a nanotube in the center, the mechanism of formation of this structure does not proceed by incorporation of a nanotube into a micelle, but rather by a two-step adsorption that ends up in the formation of a surfactant monolayer.

1. Introduction

The critical need for cost-effective methods to readily disperse single-walled carbon nanotubes (SWNT) has motivated numerous researchers to investigate the solubility of nanotubes in a variety of solvents. The insolubility of SWNT in either water or organic solvents has prompted research efforts focused on nanotube functionalization combined with dissolution in organic solvents, or mixtures of organic solvents and water. The first solubilization attempts made use of the possibility of shortening the SWNT by acid attack in concentrated sulfuric−nitric mixtures.[1] These aggressive treatments were shown, however, to introduce a significant number of defects along with amorphous carbon that is generally undesirable.[2] Moreover, a reduction in size makes short nanotubes unsuitable for many applications that are based on the nanotube length.

At the same time, some functionalization methods showed promise for the enhancement of solubilization of SWNT in organic solvents. In a popular method developed by Haddon et al.,[3] the nanotubes are dissolved in chloroform, benzene, toluene, or other organic solvents after derivatization with thionyl chloride and octadecylamine. Alternative approaches make use of the partial oxidation of SWNT, followed by sidewall reactions with fluorine,[4] alkanes,[5] or diazonium salts,[6,7] or by ionic functionalization.[8] Other groups opted for the attachment of soluble polymers to SWNT by various methods.[9]

Despite this significant progress in SWNT suspension in organic solvents, the interest in applications that require water-soluble SWNT is growing. Water dispersions of SWNT will have important implications in fields such as biochemistry and biomedical engineering, in which organic solvents cannot be used due to evident incompatibilities with living organisms. Most recently, water-soluble SWNT started to become feasible by functionalization with amines[10,11] and DNA adducts.[12,13] However, it has been demonstrated that surface modifications after functionalization can affect the inherent electrical, mechanical, and optical properties of the nanotube.[14,15] Thus, major attention is being directed at the study of surfactants, which can successfully suspend carbon nanotubes without the formation of chemical bonds. Moreover, of paramount importance is the demonstration that surfactants have the ability to break up the SWNT bundles typically obtained from most production processes and stabilize individual nanotubes.

In other applications, the tensile strength and the stiffness of SWNT are the desired properties. In these cases, it is important to separate individual nanotubes from the bundles to maximize the effect of the intrinsic mechanical properties of the SWNT. For example, in the case of polymer composites, surfactant

* Corresponding author. Email: resasco@ou.edu.
[†] University of Oklahoma.
[‡] SouthWest Nanotechnologies.

10.1021/jp0365099 CCC: $25.00
Published on Web 11/11/2003

dispersions of SWNT may facilitate the incorporation of individual nanotubes into the matrix for reinforcement of the composite materials. In addition, the surfactant molecules could potentially serve as the link between the nanotubes and the polymer, providing stronger hydrophobic interactions that will enhance a more intimate contact at the filling−matrix interface. We have recently made efficient use of surfactants to produce polymer/SWNT composites by in situ polymerization in a surfactant-assisted miniemulsion system.[16]

In a recent study, Islam and co-workers[17] observed that sodium dodecylbenzenesulfonate (NaDDBS) is an effective surfactant to solubilize carbon nanotubes prepared by the HIPCO method. In this paper, we have investigated in detail the interactions of this anionic surfactant with purified nanotubes prepared by our own CoMoCAT synthesis method.[18] From the analysis of the effect of important parameters such as pH, surfactant concentration, nanotube concentration, and sonication time, we have developed a simple model for the nanotube−surfactant interaction. Also, of particular importance for practical applications, we have quantified the maximum concentrations of SWNT that can be effectively suspended under various experimental conditions.

2. Experimental Section

2.1. Nanotube Materials and Purification Procedure. The SWNT used in this study were obtained by a catalytic chemical vapor deposition method, developed by our group, which results in high selectivities for SWNT formation. This method, which we call CoMoCAT, employs a silica-supported Co−Mo catalyst.[18] The carbon product obtained in this method depends on the Co:Mo ratio and on the catalyst treatments that precede nanotube growth.[19] Adjustment of these parameters allows for fine control over the form of the active catalyst clusters, and therefore of the nanotube structures.[20] The nanotubes used in this study have an average diameter of 0.8 nm.[21]

The CoMoCAT synthesis was conducted in a fluidized bed reactor over a silica-supported bimetallic CoMo catalyst, prepared from cobalt nitrate and ammonium heptamolybdate precursors. The total metallic loading in the catalyst was 2 wt %, with a Co:Mo molar ratio of 1:3. Before exposure to the CO feedstock, the catalyst was heated to 500 °C in a flow of gaseous H_2 and further heated to 850 °C in flowing He. Then the CO disproportionation was carried out under a flow of pure CO at 5 atm total pressure. The SWNT grown by this method remained mixed with the spent catalyst, containing the silica support and the Co and Mo species, which were eliminated by two different purification methods.

To determine the influence of the different purification treatments on the surface chemistry of SWNT, two different methods, basic and acidic, were used in the silica-removal process. Prior to the removal of the silica, the raw material was placed in an oven at 250 °C for 10 h to oxidize the Co and Mo species remaining in the product, followed by bath sonication in hydrochloric acid (38% pure) to remove the metal oxides. The solid material was then thoroughly rinsed in Nanopure water until the pH returned to neutral, as tested with pH-indicator paper. Once the metals had been eliminated, the silica support was removed by dissolution. In this step, an acidic treatment and a basic treatment were employed for comparison. In the first case, the composite was ground and added to hydrofluoric acid (∼33% pure) in an ultrasonication bath (Cole Parmer, 168 W, 50−60 Hz) for 3 h. The hydrofluoric acid was removed by repeatedly washing with Nanopure water until the pH returned to neutral. Similarly, a second batch of composite was put in contact with 10 M sodium hydroxide for 3 h. Again, several rinses were applied until a neutral pH was reached.

To analyze the surface changes caused by the two purification methods, the HF-treated and NaOH-treated SWNT were analyzed by X-ray photoelectron spectroscopy (XPS). XPS data were recorded on a Physical Electronics PHI 5800 ESCA system with a background pressure of approximately 2×10^{-9} Torr. The electron takeoff angle was 45° with respect to the sample surface. An 800-μm spot size and 23 eV pass energy were typically used for the analysis. The binding energies were corrected by reference to the C(1s) line at 284.8 eV. Quantification of the surface composition was carried out by integrating the peaks corresponding to each element with aid of the Shirley background subtraction algorithm, and then converting these peak areas to atomic composition by using the sensitivity factors provided for each element by the PHI 5800 system software.

The surface area of SWNT was measured by N_2 adsorption at 77 K following the BET method with an ASAP 2010 instrument from Micromeritics. Prior to the adsorption of nitrogen, the samples were degassed at 250 °C for 24 h.

2.2. Determination of Points of Zero Charge. Generally, water−solid interfaces acquire a net charge of a particular sign to maintain electrical neutrality with the surface. The structure of this electrical double layer depends on the pH of the medium and the type and amount of electrolyte present. The PZC or *point of zero charge* is defined as the pH at which the surface exhibits a net surface charge of zero. At pH values below the PZC, the substrate becomes protonated and exhibits a positive net charge on the surface. In contrast, the net surface charge turns negative at pH values above the PZC. Acidic surfaces, like silica, tend to have very low PZC values (e.g., PZC of $SiO_2 \sim 3$), whereas basic metal oxides such as magnesia present higher PZCs (e.g., PZC of MgO ∼ 11).

Since the purification method may modify the surface chemistry of SWNT, we wanted to determine the PZC values for acid-treated as well as for base-treated SWNT. The PZC were obtained by the following simple technique. Two series of 10 mL water vials were prepared with initial pH values in the range of 1−10. These pH values were adjusted by addition of concentrated hydrochloric acid for the acidic range and sodium hydroxide for the basic range, making use of a Orion Model 310 pH meter. About 1.5 mg of either HF-treated or NaOH-treated SWNT was placed in each vial of the series and left overnight to reach equilibrium at 25 °C. The equilibrium (final) pH was then measured and plotted against the initial pH for each series. The PZC can be readily obtained from the point at which the initial pH vs final pH curve crossed the $y = x$ line on the graph.

2.3. Surfactant Adsorption Isotherms. The adsorption of pure surfactants and surfactant mixtures onto inorganic and organic surfaces has been widely studied.[22−27] This phenomenon usually depends on the chemical characteristics of the solid, the nature of the surfactant molecules, and the nature of the solvent. It has been extensively demonstrated that the main driving forces for adsorption of ionic surfactant molecules on charged surfaces are the Coulombic attractions between the surfactant heads and the charged surface groups from the solid, and the hydrophobic bonding between the surfactant tails.[22−25] Therefore, to enhance the adsorption of surfactants onto inorganic substrates, the surface charge can be manipulated by adjusting the pH in reference to the point of zero charge (PZC) of the solid. For strong adsorption of anionic surfactants, the substrate should exhibit a positive charge, which can be achieved by lowering the pH below the PZC. By contrast, for cationic

surfactants, the pH should be adjusted above the PZC. However, the mechanism by which surfactants adsorb onto hydrophobic surfaces differs, depending upon the hydrophobic interactions between the surfactant tails and the hydrophobic surface of the substrate. To enhance the formation of aggregates on the solid surface, the concentration of surfactant must be adjusted to an optimum, when the interactions between adsorbed molecules and molecules in the bulk become dominant.[28] Above the cmc (critical micelle concentration), micelles begin to form in the supernatant solution so that an adsorption plateau is reached.

Based on the interesting solubilization capabilities of sodium dodecylbenzenesulfonate (NaDDBS) for carbon nanotubes, demonstrated by Islam et al.,[17] a full study of the interactions between SWNT and NaDDBS has been performed. To fully understand how NaDDBS solubilizes hydrophobic carbon nanotubes, measurements of the adsorption isotherm of NaDDBS on purified carbon nanotubes have been conducted at 25 °C, at two different pH values, 4 and natural. To determine whether formation of surfactant aggregates occurs on the SWNT, and in what quantity they form, a fixed amount of purified SWNT (0.17 mg/ mL) was put in contact with 20 mL of DDBS solutions of known initial concentrations. The dispersions were ultrasonicated for 1 min with a horn dismembrator (Fisher Scientific, 600 W, 20 kHz) and left undisturbed for 12 h to ensure equilibrium.

After equilibrium was reached, the liquid was collected by filtration of the resulting solution. Depending on the concentration this solution may or may not have micelles. Therefore, one can decide whether to let the surfactant micelles remain with the solid or the liquid phase, by simply changing the pore size of the filter used. In this case, since it is possible that SWNT can act as molecular sieves and inhibit the free flow of micelles through the filtration system, we decided to retain the micelles together with the nanotubes. Accordingly, 2.5 mL disposable centrifuge cellulose acetate microfilters of 10-kDa cutoff (from Sartorious) were employed, which retain 100% of the NaDDBS micelles. Thus, the filtered liquid only contained free surfactant, i.e., surfactant that is not attached to the nanotubes nor is forming micelles. The concentration of free surfactant in the liquid was quantified by a UV spectrophotometer (UV-2100, Shimadzu) operating at a wavelength of 225 nm. From the measured concentration of free surfactant, the amount of NaDDBS adsorbed on the SWNT surface was determined. Two plots with important information are obtained. One is the concentration of free surfactant as a function of the amount of surfactant added to the system (Figure 3). As shown in this figure, the free surfactant concentration increases up to the onset of micelle formation, i.e., the critical micelle concentration (cmc), at which point it remains unchanged with further addition of surfactant. The second plot is the adsorption isotherm, which derives from these data and is shown in Figure 4. This plot only includes the data of Figure 3 before the plateau is reached. Since the plateau corresponds to the concentration of free surfactant at which micelles start to form, Figure 4 only includes data in which no micelles are present. To calculate the amount of adsorbed surfactant shown in Figure 4 as a function of equilibrium concentration, we subtracted the free surfactant concentration from the total added surfactant concentration.

The driving force for the adsorption of ionic surfactants on solid surfaces is generally the Coulombic attraction between the headgroups of the surfactant and the surface of opposite charge. Depending whether the pH of the medium is below or above the PZC of the solid, the surface charge becomes positive or negative, respectively. Thus, the adsorption of the surfactant can be enhanced with the appropriate pH. To explore whether this is also the case for SWNT, a series of adsorption experiments were run at different pH values, covering both the acidic and basic regions.

The feed concentration of NaDDBS was fixed at 0.03 and 0.6 mM (0.025 and 0.5 times the cmc at 60 °C, respectively)[29] to account for the effect of the concentration of surfactant. The concentration of SWNT was kept constant in all the vials at 0.17 mg/mL. The initial pH was adjusted to 2, 4, 6, 8, and 10 with concentrated hydrochloric acid and sodium hydroxide, respectively. After allowing the system to reach equilibrium, the supernatant was collected with a cellulose acetate microcentrifuge filter and the free surfactant concentration was determined by UV−vis spectrophotometry.

2.4. Surface Tension Measurements. To verify that the interaction of SWNT with the surfactant is responsible for changes in the liquid concentration of NaDDBS, the dependence of the cmc value on the presence of various amounts of purified SWNT was determined from surface tension (γ) measurements as a function of surfactant concentration. Typically, the surface tension decreases with surfactant concentration up to the point at which the surface tension becomes constant. This point is the critical micelle concentration (cmc): when micelles begin to form in solution, the concentration of surfactant at the air−water interface remains constant even when the amount of added surfactant increases.

Purified SWNT were added in concentrations of 0.017 and 0.17 mg/mL onto solutions of varying concentrations of NaDDBS in deionized water. The suspensions were then horn sonicated and poured into a glass container previously washed in acid and thoroughly rinsed with deionized water. A Krus Processor Tensiometer K12 was operated under the Wilhelmy plate technique.[30] The platinum slide was washed in acid, rinsed with deionized water, and brought to incandescence in a flame after every measurement to remove any residue of SWNT or surfactant. Surface tension values were measured at 30 °C, controlled by an external water jacket. Values of the surface tension were then represented against the logarithm of the total surfactant concentration to obtain the breakpoint, which corresponds to the effective cmc. From the initial slope, the surface excess (Γ) at the air−water interface can be calculated from the Gibbs equation.[30]

2.5. Nanotube Suspendability in Surfactant Solutions. The formation of stable suspensions of SWNT is a critical target in the development of practical applications of this valuable material. As mentioned above, the successful incorporation of nanotubes into practical materials relies on the capability of breaking up the bundles into individual nanotubes and keeping them in homogeneous and stable suspensions. To facilitate the study of suspension stability, we have developed the following method for quantification of the fraction of SWNT suspended in solutions at either varying surfactant concentration or varying SWNT concentration. In the first set of experiments, surfactant solutions with concentrations ranging from 0.065 to 4 mM were prepared in 20 mL vials. Fixed amounts of purified SWNT were added to each vial, resulting in a fixed concentration of 0.06 mg of carbon/mL. Because the sonication time was believed to play an important role in the final dispersions, two sonication times were compared, 1 and 20 min. After subsequent centrifugation, the supernatant was collected in a separate vial, ensuring that no precipitate of nanotubes was incorporated in the final solution. To evaluate the fraction of suspended SWNT, the final solutions were analyzed under the UV spectrophotometer at 800

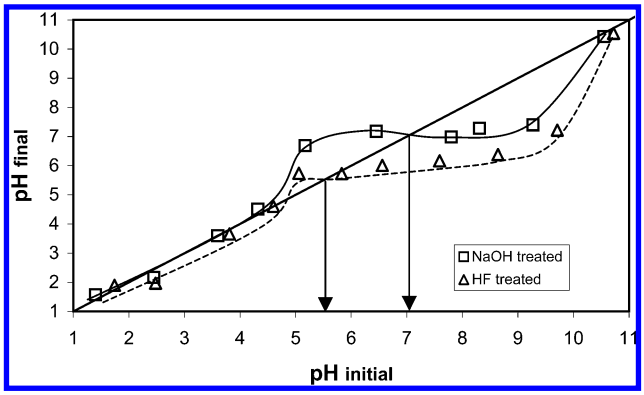

Figure 1. Determination of PZC for SWNT after NaOH treatment (PZC = 7.0) and HF treatment (PZC = 5.5).

nm. At this wavelength, the surfactant does not interfere with the UV absorption of the nanotubes.

In the second set of experiments, varying amounts of SWNT were added to 20 mL of NaDDBS solutions of fixed concentrations of 0.12 and 1.2 mM (i.e., 0.1 and 1 times the cmc at 60 °C, respectively).[29] The concentrations of SWNT varied from around 0.01 to 0.25 mg of SWNT per milliliter of solution. Each vial was first horn sonicated for 1 min, and then centrifuged at 3400 rpm for 25 min. As in the first set of experiments, the amount of suspended SWNT was evaluated by absorption at 800 nm.

To further investigate the role of the time of sonication, two series of SWNT−NADDBS solutions (SWNT 0.27 mg/mL, NaDDBS 0.25 cmc and 1 cmc) were prepared and horn sonicated for different times ranging from 1 to 125 min. The resulting dispersions were examined under UV−vis spectroscopy to quantify the final concentration of suspended nanotubes. To determine whether vigorous sonication can result in damage of the SWNT, the liquid suspensions were further characterized by Raman spectroscopy and NIR absorption spectroscopy. The Raman spectra were obtained on a Jovin Yvon-Horiba LabRam 800 equipped with a CCD detector and with three different laser excitation sources having wavelengths of 632 (He−Ne laser) 514, and 488 nm (Ar laser). Typical laser powers ranged from 3.0 to 5.0 mW. The G/D band ratios were calculated in each case and used as a measurement of the presence of disordered carbon and to monitor any nanotube destruction caused by the severe sonication.

3. Results and Discussion

3.1. Point of Zero Charge. The curves of final pH as a function of initial pH for purified nanotubes in water showed, as expected, a crossing point of the $y = x$ line at a final pH that, as described above, corresponds to the PZC of each sample. As shown in Figure 1, the NaOH-treated SWNT sample exhibited a PZC of around 7 while the HF-treated SWNT sample had its PZC at a pH of about 5.5. These results indicate that HF-treated SWNT samples are negatively charged when exposed to pH values higher than 5.5, while the NaOH-treated sample only becomes negative above pH 7. These findings are in good agreement with what Sun et al.[31] have previously observed on multiwalled nanotube (MWNT) samples. They measured the zeta potential of the as-produced and chemically modified MWNT at different pH values. They found that the zeta potential of pristine nanotubes was zero at pH 5.8, but after treatment of the SWNT in NH_3 at 600 °C, the PZC shifted to 9.8. In another report[32] the same authors indicate that acid-treated nanotubes exhibit negative zeta potentials in a pH range from 2 to 12. They propose that the permanent negative charge is due to the presence of carboxylic acid groups resulting from the strong acid treatment. It is possible that a high density of carboxylic acid groups may shift the PZC to pH values even lower than the minimum pH used in that study. In another study, Sano and co-workers[33] also observed carbon nanotubes with a net negative charge after cutting them by severe acid/peroxide etching. Yet, the effect of the pH was not taken into consideration in that study and the measurement of the zeta potential was presumably carried out at a pH value above the PZC. More recently, another research group[34] compared the PZC of carbon nanotubes before and after strong oxidization with nitric acid, hydrogen peroxide, and potassium permanganate. They found that the PZC of SWNT decreased with the degree of oxidation, which varied from one oxidating agent to another.

The observed changes in PZC can be explained taking into account that proton adsorption occurs on the nanotube surface when the pH of the surrounding medium is below the PZC. By contrast, release of protons from the surface occurs when the pH is higher than the PZC. If the concentration of OH^- is further increased, negative charges are generated on the surface. In the case of NaOH-treated SWNT, chemisorption of basic Na^+ on the surface shifts the PZC to higher values, while on the HF-treated SWNT the presence of chemisorbed fluoride anions shifts the PZC to lower values. Similar upward and downward shifts in PZC are typically observed when basic ions or halogens are added to inorganic solids. For example, it has been shown that small amounts of Na^+ and K^+ can significantly increase the PZC of silica.[35−37] Similarly, the presence of chloride on alumina has been seen to lower the PZC from 8 to 6.[38]

The PZC measurements were complemented by X-ray photoelectron spectroscopic (XPS) analysis to quantify the surface concentration of the different elements that may be left on the SWNT sample as a result of the particular pretreatment method. The XPS surface analysis results were in good agreement with the observed trends in PZC. As illustrated in Figure 2A, the presence of fluorine is clearly evident on the SWNT surface after the HF treatment. At the same time, the NaOH treatment resulted in the presence of a small percentage of sodium on the SWNT surface, as shown in Figure 2B.

Knowing the surface charge of the nanotubes in different media is critical not only for understanding their interactions with ionic surfactants, but also for other important applications. For example, dispersing metals on the surface of nanotubes has great implications in applications in heterogeneous catalysis as well as fuel cell electrocatalysts. SWNT can be used as catalyst supports where the electrical charge could be the driving force for the impregnation of metallic catalysts by Coulombic attraction.

Although the PZC measurements demonstrated the presence of different surface charges under different conditions, it is not immediately obvious that these charges can dominate the adsorption process over the similarly important hydrophobic interactions that are certainly possible when a surfactant interacts with a hydrophobic surface as the one of SWNT. The importance of SWNT−aromatic ring interaction has been clearly illustrated by Chen et al.[39] Since the hydrophobic tail of the NaDDBS contains an aromatic ring, its interaction with the nanotube surface may indeed by significant.

3.2. Surfactant Adsorption Isotherms. Isotherms of NaDDBS adsorption on purified SWNT were conducted above and below the PZC of HF-treated SWNT. First, the free surfactant concentration was represented against the total added surfactant,

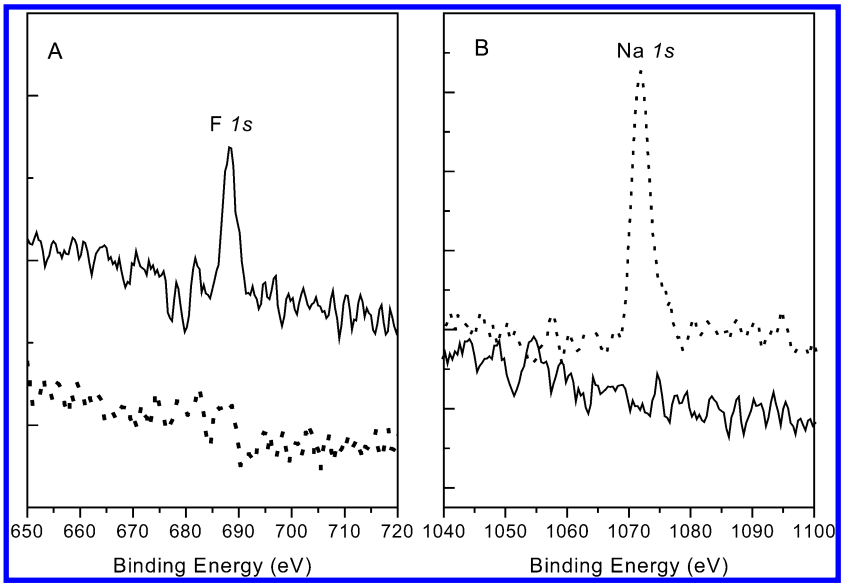

Figure 2. XPS spectra for F(1s) and Na(1s) levels. HF-treated SWNT (solid line) and NaOH-treated SWNT (dotted line).

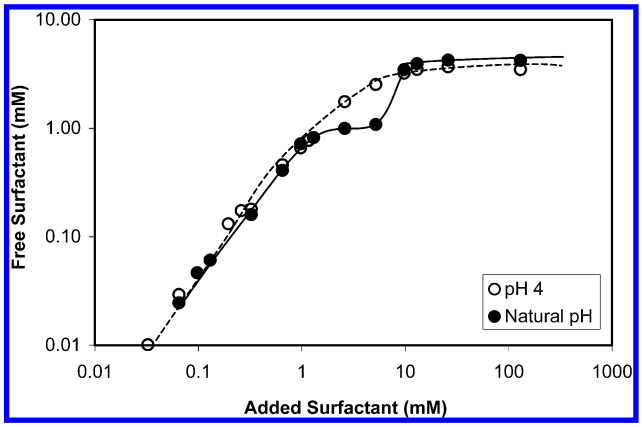

Figure 3. Equilibrium concentration of free NaDDBS as a function of added surfactant after adsorption on 0.17 mg of SWNT/mL at 25 °C.

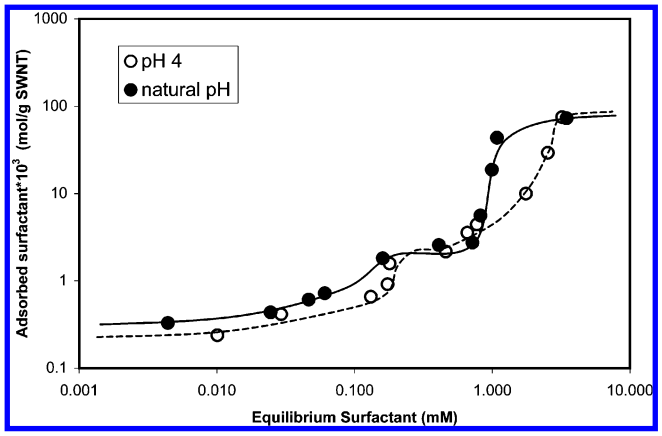

Figure 4. Adsorption isotherms of NaDDBS on HF-treated SWNT (PZC = 5.5) at pH 4 and natural pH at 25 °C.

as shown in Figure 3, which is the data directly obtained from UV−vis spectroscopy. From Figure 3 we were able to determine when micelles started to form. This is the point at which the concentration of free surfactant in the supernatant remained constant (∼3.4 mM). At this concentration maximum adsorption was reached, and the free surfactant concentration did not further change. The actual isotherms presented in Figure 4 were calculated by subtracting the free surfactant from the added surfactant up to the point at which the plateau was reached. Therefore, the last point in the isotherm corresponded to a free surfactant concentration of around 3.4 mM.

The shapes of both isotherms seem to indicate a two-step mechanism of adsorption, as evidenced by the steps in the curves. At concentrations of surfactant below 1 mM, both curves grow in parallel until, for the isotherm at natural pH, there is a sudden increase in adsorbed surfactant. As expected, both isotherms reach the saturation plateau at the same maximum adsorbed concentration. The equilibrium concentration of surfactant in the liquid phase at this point corresponds to the plateau, which in the presence of SWNT may differ from the cmc of the pure surfactant solution. The fact that both isotherms conducted below and above the PZC of the nanotubes show no significant differences, particularly at low concentrations, suggests that Coulombic attractions do not govern the adsorption process. If that were the case, the adsorption at low surfactant concentrations should be more extensive when conducted below the PZC than with the natural pH. At low pH the negatively charged headgroups should be more attracted by the positively charged surface. Therefore, this absence of differences indicates that, at low surfactant concentrations, the molecules interact with the nanotubes, most probably resting with their aromatic-containing tails parallel to the surface due to strong van der Waals attraction with the structure of the nanotube walls. According to the classical reorientation model, at such a small concentration of surfactant, the limitation of space on the surface is minimum, and the surfactant adsorbs in a "head-to-tail" arrangement parallel to the surface.[40] However, when the concentration of surfactant is high enough, the "tail-to-tail" hydrophobic interactions among the surfactant alkyl chains become dominant and the aggregation number increases. Thus, we expect surfactant molecules to orient "tails on" for concentrations above 0.1 mM, until the surface becomes saturated with surfactant molecules. Both isotherms, the one at natural pH and the one at pH 4, show saturation amounts of adsorbed surfactant on the same order of magnitude, i.e., 7.5×10^{-2} mol of surfactant per gram of SWNT.

According to the literature, the aggregation number of adsorbed surfactants is highly dependent on the surface morphology that acts as a template, and also on the structure and length of the surfactant alkyl chain.[41] In a very interesting calorimetric study, Király et al.[42−44] demonstrated, by a series of adsorption isotherms of surfactants on graphite, that the

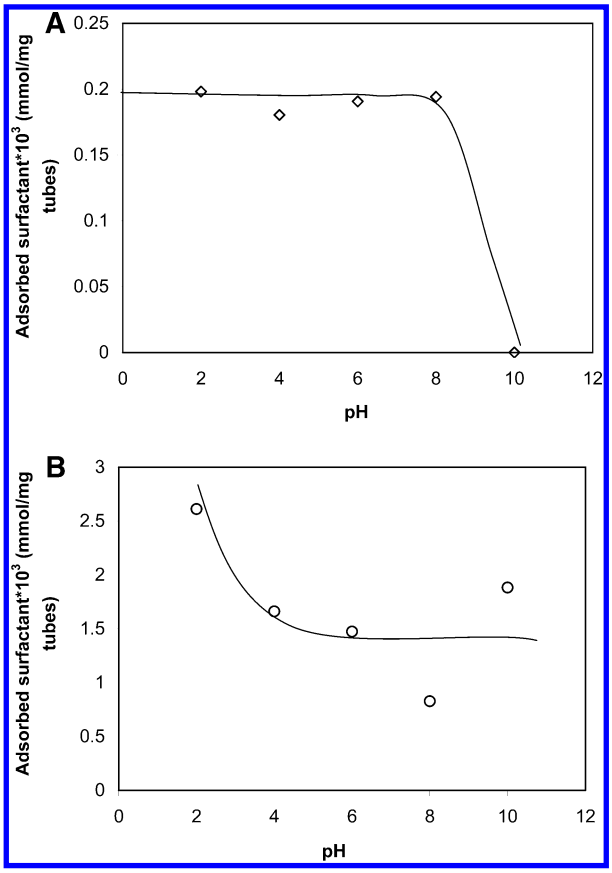

Figure 5. (A) Effect of pH on adsorption of NaDDBS, 0.025 cmc, on HF-treated SWNT at 25 °C. (B) Effect of pH on adsorption of NaDDBS, 0.5 cmc, on HF-treated SWNT at 25 °C.

maximum adsorption was obtained when the alkyl chain length was increased. Similarly to what we have observed here, the adsorption on graphite was driven by the hydrophobic interactions exclusively. Furthermore, they observed similar adsorption behavior with a cationic (C_{12}TAB) surfactant and an anionic (SDeS) surfactant, as well as with various polyethoxylated nonionic surfactants. These results indicated the hydrophobic nature of the interactions between the surfactant molecules and the graphite surface.

To verify that anionic surfactant adsorption on SWNT does not respond to changes in the pH, additional adsorption measurements were performed in a wider pH range at a fixed initial NaDDBS concentration of 0.03 mM. Figure 5A shows that, in agreement with the previous result, further changes in pH did not alter the extent of NaDDBS adsorption up to pH 10, at which the surfactant adsorption suddenly dropped to zero. This drop can be due to the repulsion generated between the negative heads of the surfactant and the excess negative charge generated on the SWNT surface well above the PZC, which overcomes the attraction hydrophobic forces between the surfactant tail and the nanotube. Conversely, when the concentration of surfactant is increased to 0.5 times the cmc (Figure 5B), the adsorption appears to be slightly enhanced at very low pH, at which the concentration of H^+ on the surface is high enough to dominate the interactions with the negatively charged headgroups. In conclusion, it seems that only far from the PZC the Coulombic forces of attraction or repulsion can overcome the strong hydrophobic interaction between the surfactant and the nanotubes.

3.3. Surface Tension. Surface tension measurements provided further evidence for the surfactant adsorption on SWNT. As mentioned earlier, the effective cmc of the system can be

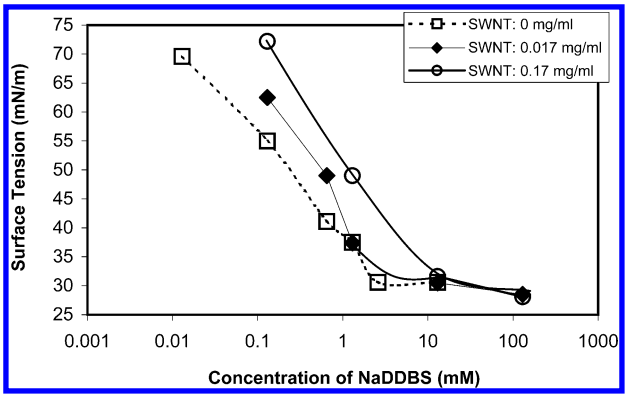

Figure 6. Surface tension measurements of NaDDBS solutions in the presence of NaOH-treated SWNT at 30 °C.

determined from the breakpoint in the $\gamma-\log C$ curve. For example, it is typically observed that, in the presence of organic solutes, the cmc is reached at lower concentrations because the formation of micelles in solution is enhanced by the solubilization of organic solutes in the hydrophobic core of the micelles. By contrast, when a surfactant adsorbs on a surface, it can be expected that higher concentrations will be needed to reach the cmc because the amount adsorbed is removed from solution. In fact, Figure 6 shows that, in the presence of the nanotubes, the breakpoint is reached after adding about 5 times more surfactant than when the nanotubes were not present. In the presence of 0.17 mg/mL SWNT, the concentration of added surfactant had to be increased to about 13 mM compared to 2.6 mM. This shift indicates that the surfactant is being adsorbed by the carbon nanotubes, causing the effective concentration in the bulk to decrease. Thus, extra amounts of surfactant have to be added before formation of micelles can occur. Actually, if we subtract the added concentration of surfactant at which the cmc is reached for pure NaDDBS from the same concentration in the presence of nanotubes and we divide by the amount of nanotubes in the system, we obtain that the total adsorbed surfactant was 6.1×10^{-2} mol of NaDDBS per gram of SWNT. This result is in perfect agreement with the adsorbed surfactant obtained from the adsorption isotherms (i.e., 7.5×10^{-2} mol/g SWNT).

To link the surface characteristics of the nanotubes to the observed cmc shifts, a series of surface tension measurements were conducted with SWNT pretreated under acidic and basic attack. For this comparison, equal amounts of NaOH-treated and HF-treated SWNT, as well as annealed HIPCO SWNT,[45−47] were added to a series of NaDDBS solutions of varying concentrations. The surface tensions for each of the samples are compared in Figure 7 as a function of the initial concentration of surfactant. Interestingly, three overlapping curves were obtained, with their breakpoints at practically the same surfactant concentration. The conclusion of this comparison is that the net amount of adsorbed surfactant was essentially the same in all cases. This constant adsorption value indicates that differences in the surface chemistry of the purified SWNT play a minor role in the structure of the adsorbed surfactant that results at high surfactant concentrations.

3.4. Model for the Surfactant−Nanotube Interaction. Until now, only a few studies have been dedicated to the development of models that explain the role of surfactants in the dispersion of SWNT. In a recent publication, researchers at Rice University[48] have proposed that SWNT are solubilized inside SDS (sodium dodedyl sulfate) columnar micelles in aqueous solution as a result of energetic sonication of the mixture. It is important to note here that, under the experimental conditions employed

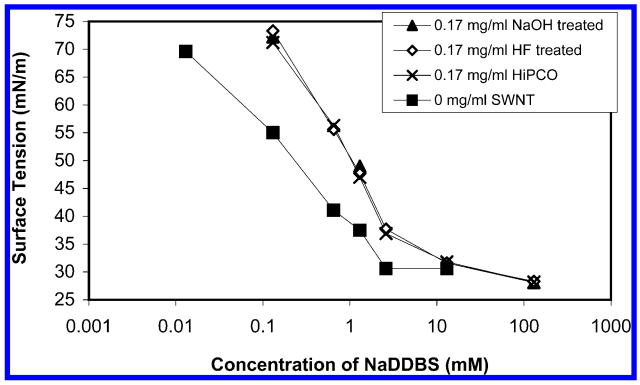

Figure 7. Surface tension measurements of NaDDBS solutions in the presence of NaOH-treated, HF-treated, and HIPCO SWNT at 30 °C as a function of added surfactant.

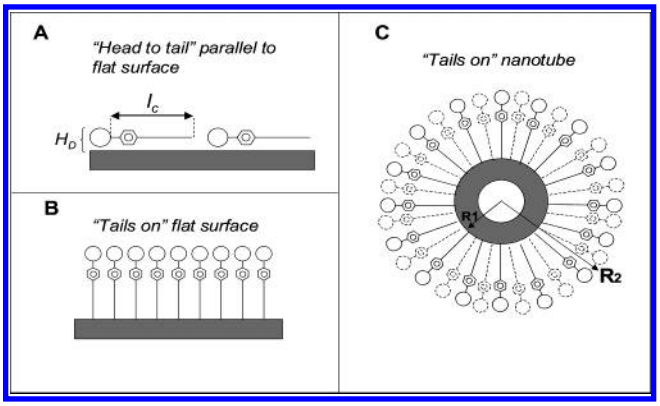

Figure 8. Model for the surfactant−nanotube interaction. Head cubic packing density = 1.45 molecules/nm^2. Head diameter (H_D) = 0.69 nm. Chain length (l_c) = 1.5 + 1.265n (Å). n = number of carbons; l_c = 24.27 (Å).

in that study, only spherical micelles are possible. Therefore, columnar micelles can only be formed as a result of the interaction with the nanotube. In a subsequent investigation, the same group of authors improved their model by recognizing the importance of the surfactant adsorption in the nanotube debundling process that leads to surfactant-stabilized individual nanotubes.[49] In fact, our experimental evidence demonstrates that SNWT are not solubilized inside an existing cylindrical micelle, but rather the surfactant adsorbs on the external surface of the nanotubes. As a result, the final nanotube−surfactant aggregate takes indeed the appearance of a cylindrical micelle with the nanotube resting in the interior. The initial interaction is probably one in which the surfactant lies parallel to the surface, as the surface coverage increases, and before forming a monolayer, the surfactant molecules stand up in a "tails on" configuration until the adsorption reaches equilibrium. This is also supported by the abrupt increase of almost 2 orders of magnitude in the adsorption density clearly depicted in Figure 4. The formation of such a stable monolayer should result in the stabilization of individual tubes readily suspended in solution.

To verify our hypothesis, we have first calculated the necessary number of NaDDBS molecules to complete a full monolayer on 1 m^2 of surface area of nanotubes of 0.8 nm in diameter. Of course, this is an approximation, since carbon nanotubes are usually produced within a size distribution range, typically characteristic of the production method.[50]

In our current model, we propose a monolayer of adsorbed surfactant with a vertical orientation with the anionic headgroups directed outward to the aqueous phase. This is not the surfactant structure that one may expect to obtain on a flat carbon surface. In fact, many studies of surfactant adsorption on graphite[42−44,51] indicate that surfactants adsorb forming hemicylindrical surface aggregates running in long grains, parallel to each other along the surface. In this hemicylinder configuration, the inner surfactant molecules lie flat on the surface while those in the center of the aggregate stick heads up, vertically into the solution, with a fanlike appearance. However, based on geometric grounds, this would be an unlikely configuration for the surfactant/nanotube due to the high curvature of the nanotube surface, which would make the fanlike structure unstable. The curvature of the nanotubes would rather force the surfactant molecules to aggregate as spherical micelles threaded along the nanotube. However, the electrical charge repulsions between heads and the inherent difficulty of packing such large molecules on nanotubes of relatively small diameters suggest that the adsorbed monolayer is the most likely configuration. The schematic model that we propose, illustrated in Figure 8, compares the number of NaDDBS molecules required to cover a flat graphite sheet with the carbon nanotube that results from rolling up the graphite sheet with a diameter of 0.8 nm. We can use the experimental surfactant packing density obtained below from eq 3 (1.45 molecules/nm^2). NaDDBS is an isomeric mixture of chain lengths with an average alkyl chain length shorter than 12 carbons, due to the different points of attachment of the phenyl ring along the alkyl chain. As a first approximation, we have considered the fully extended length of the alkyl chain, which was calculated from the following empirical equation:[29]

$$l_c = 1.5 + 1.265n \quad (\text{Å}) \tag{1}$$

where n is the number of carbons in the alkyl chain.

If we hypothetically open a carbon nanotube of radius R_1, we obtain a graphite sheet of width equal to the perimeter of the nanotube, $P_1 = 2\pi R_1$. Let us call m the number of molecules adsorbed per unit area on this sheet. The maximum packing number will be limited by the size of the headgroups, assuming vertical orientation perfectly parallel to each other. However, if we distribute the same number of molecules on the surface of a nanotube of radius R_1, the curvature increases the distance between headgroups so that more molecules can seat on the surface. The new effective perimeter will be given by

$$P_2 = 2\pi R_2 = 2\pi(R_1 + l_c + H_R) \tag{2}$$

where R_2 corresponds to the radius of the circumference described by headgroups of the surfactant molecules seating on top. Thus, the increase in available area for the arrangement on the nanotube surface will be given by the ratio of P_2/P_1. Substituting the data given above into eq 2, we obtain that the curvature of the nanotube introduces a multiplying factor of about 8, meaning that a carbon nanotube of 0.8 nm in diameter[52] can hold almost 8 times more molecules than a flat graphite sheet with a width equal to the perimeter of that tube. Based on the estimated packing density of surfactants on a flat surface (1.45 molecules/nm^2), the number of moles necessary to form a complete monolayer of NaDDBS was calculated per surface area unit. The resulting value was then multiplied by 8, to account for the effect of the nanotube curvature, and the final result was 1.9×10^{-5} mol/m^2.

To evaluate the consistency between the experimental adsorption isotherms and the theoretical predictions, one needs to consider the surface area of the SWNT. Our measurement of the purified and dried SWNT sample as measured by the BET

TABLE 1: Summary of Surface Concentration of Surfactant on a Flat Interface and on Single-Walled Carbon Nanotubes as Calculated from the Model and the Experimental Results

adsorption system	estimation method	surfactant packing no. (molecules/nm^2)	surfactant adsorbed (mol/g)
	Flat Surfaces		
monolayer flat surface	calcd: van der Waals radii	2.9[a]	
saturation on flat interface	exptl: surface tension	1.45	
saturation on flat interface	exptl: adsorption isotherm	2.2[b]	2.5×10^{-4} [b]
	SWNT		
monolayer, 0.8 nm SWNT	calcd: model	11.6	3.9×10^{-2} [c]
saturation surfactant adsorption on SWNT	exptl: adsorption isotherm	22.5[c]	7.5×10^{-2}
saturation surfactant adsorption on SWNT	exptl: surface tension	18.3[c]	6.1×10^{-2}

[a] From ref 54. [b] From ref 44. [c] Assumed surface area = 2000 m^2/g.

method yielded a value of 500 m^2/g. However, it has been widely recognized[53] that BET measurements of bulk dry samples result in surface areas far lower than the theoretical external area of the nanotubes because the nanotubes are present in bundles with a large fraction of inaccessible area. This area could become accessible in the surfactant suspensions.

To confirm the packing number of the NaDDBS molecules, the area per molecule of packed surfactant was also calculated from the Gibbs adsorption equation from the surface tension curves. For a binary mixture with an ionic surfactant without added electrolyte, the number of surfactant molecules per area at the air−water interface can be obtained from the following expression:

$$\Gamma = \frac{-1}{2RT}\left(\frac{d\gamma}{d \ln C}\right) \quad (3)$$

where Γ is the surface excess in mol/m^2, γ is the surface tension in mN/m, and C is the concentration of surfactant. The average Γ values of 2.4×10^{-6} mol/m^2 for HF-treated SWNT, which corresponds to 1.45 molecules/nm^2, is in reasonably good agreement with the packing numbers obtained in previous studies. For example, the cubic packing density of the sulfonate headgroup has been calculated as 2.9 molecules/nm^2, based on its van der Waals radius.[54] Similarly, the maximum adsorption density for SDS (which has the same headgroup as NaDDBS) on alumina was found to be 1.9 molecules/nm^2.[55] The calculated and experimentally measured saturation surface concentrations are summarized in Table 1. The results show the excellent internal consistency of the experimental data and the relatively good agreement with the values predicted from the simplified model. It is interesting to note that the maximum adsorption density on SWNT is almost an order of magnitude higher than that of SnDS adsorbed on a flat graphite surface,[44] as the model predicts. It must be noted that SnDS, SDS, and NaDDBS all have the same sulfonate headgroup, which makes this comparison valid.

3.5. Suspendability of Nanotubes. A practical outcome of this study was the quantification of the surfactant ability to bring about the dispersion of SWNT and formation of stable aqueous suspensions. The concept "stability" can be defined in different ways, depending on the chosen reference. In this paper we introduce the term "suspendability", which we define as the concentration of SWNT that remains in suspension after several centrifugations for a fixed concentration of surfactant. We believe that there must be a limit in the concentration of surfactant that effectively disperses the nanotubes.

Figure 9 shows the concentration of suspended nanotubes at a feed concentration of 1 and 0.1 cmc NaDDBS, for 1 and 20 min of sonication, respectively. In all cases, a maximum fraction of suspended tubes was reached, which depended on both the

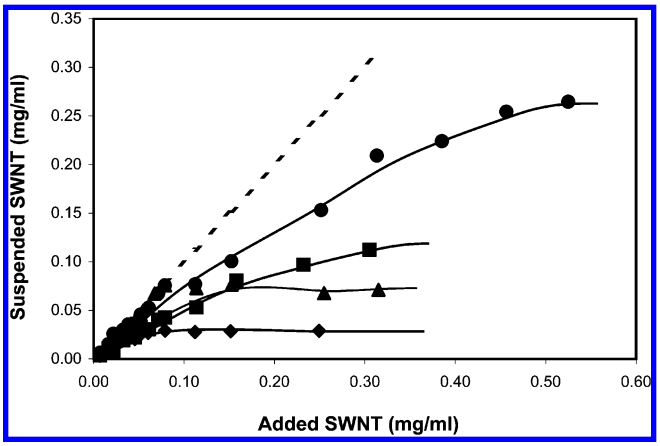

Figure 9. Determination of concentration of suspended SWNT at various concentrations of NaDDBS as a function of concentration of SWNT. Horn-sonication times are 1 and 20 min. (◆) 0.1 cmc (1 min); (■) 1.0 cmc (1 min); (▲) 0.1 cmc (20 min); (●) 1.0 cmc (20 min).

sonication time and the concentration of added surfactant. At low sonication time, the surfactant concentration had a more dramatic effect. For an added NaDDBS solution at 0.1 cmc and sonicated for 1 min, the maximum amount of SWNT that could be suspended was around 0.028 mg/mL. However, when the feed concentration of NaDDBS was increased to 1.0 cmc, the amount of suspended nanotubes greatly increased to about 0.11 mg/mL. On the other hand, when the mixture was sonicated for longer times, 0.1 cmc increased the concentration of suspended nanotubes to about 0.07 mg/mL. These maximum values are in good agreement with suspendabilities reported in previous work.[17,56] Furthermore, when the sonication time was extended for 20 min for the solution at the cmc, the concentration of nanotubes that remained stable in the dispersion increased by more than 2.5 times, i.e., 0.26 mg/mL, which confirmed that the effect of sonication is crucial in the optimization of the surfactant use.

To further analyze this behavior, the percentage of suspended nanotubes at a fixed concentration of surfactant and SWNT was represented against the sonication time. Many authors have realized that the time of sonication is a key factor in the dispersion of SWNT. Other groups have indirectly observed that functionalization needs to be preceded or followed by appropriate sonication in order to reach highly dispersed SWNT solutions.[49,57−60] According to Figure 10, we have found that it is possible to obtain a stable suspension of SWNT at a concentration of 0.16 mg/mL only when the feed concentration of NaDDBS was at the cmc and when energetic sonication was applied for at least 25 min. This result is in perfect agreement with the data shown in Figure 9, for an initial concentration of nanotubes of 0.25 mg/mL at the same sonication time (20 min). Actually, it can be seen that both curves approach each other

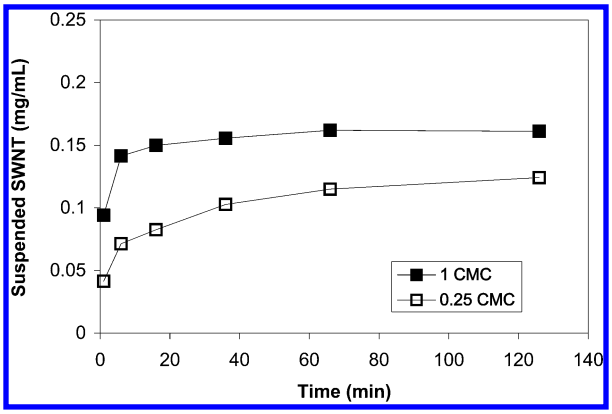

Figure 10. Effect of sonication time on suspendability of SWNT. NaDDBS concentrations are at 0.25 and 1.0 cmc. Horn dismembrator (600 W, 20 kHz).

as the sonication time increases. This trend indicates that, for a given amount of SWNT, it is possible to disperse almost the same quantity of nanotubes with 1 and 0.25 cmc if the sonication time is enough and when there is sufficient surfactant in solution to cover the surface area required for solubilization. Again, additional sonication did not seem to facilitate any further solubilization of the nanotubes.

In the case of surfactant solutions, we believe that longer sonication times favor the breaking up of the bundles, thus exposing additional surface area for the adsorption of the surfactant molecules onto the nanotubes. Evidently, there is a point at which the majority of the bundles open up. Once all nanotubes are individually dispersed, the maximum concentration of suspended nanotubes will depend on the amount of surfactant available for the solubilization. That explains why 25 min was also the time required to reach the plateau at 0.25 times the cmc. This was the time needed to break the bundles for that particular concentration of SWNT. In this case, however, the maximum concentration of solubilized nanotubes was around 0.1 mg/mL, which was limited by the surfactant available in solution.

Nevertheless, we were concerned about the occurrence of possible destruction of some of the nanotubes after horn sonicating for such long times, which would lead to amorphous carbon that would be counted as suspended nanotubes. Islam et al.[17] reported that, after horn sonication of NaDDBS−SWNT solutions for more than 1 h, the yield of individual nanotubes in solution varied with the sonication technique because of possible fragmentation after long horn sonication. There are several studies that demonstrate the effect of sonication time on the SWNT size distribution as well as on the conversion of the SWNT into amorphous carbon.[58−62] Part of the reason nanotubes do not precipitate after severe sonication is that the length of the nanotubes is being cut and shorter SWNT are much easier to disperse. However, making use of Raman spectroscopy and NIR absorption, we have shown that within the sonication times employed in this study (up to 125 min) no significant nanotube destruction was detected. Raman spectroscopy provides a semiquantitative measure of the degree of nanotube destruction by the relative size of the D band (disordered carbon) and the G band (graphite tangential). The variation of the quality parameter [1 − (D/G)] with the sonication time as obtained from the Raman spectra of sonicated the NaDDBS−SWNT solution series is illustrated in Figure 11. The D band appears almost flat at all sonication times, and its intensity does not vary with the sonication time. Only at 125 min of sonication was a slight but not significant increase observed, which results in a lower

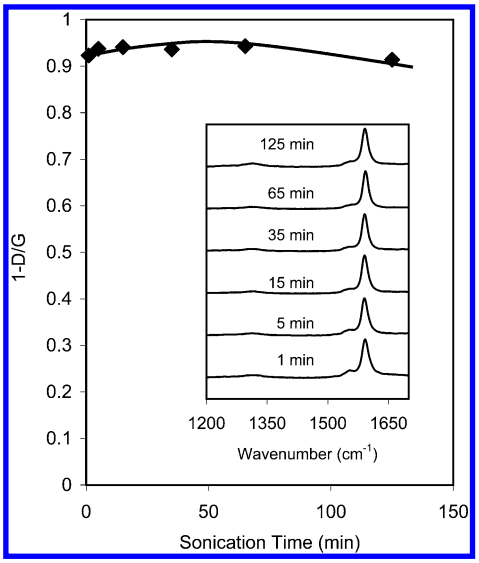

Figure 11. Raman spectra and values of the [1 − (D/G)] parameter for NaDDBS−SWNT solutions after various sonication times.

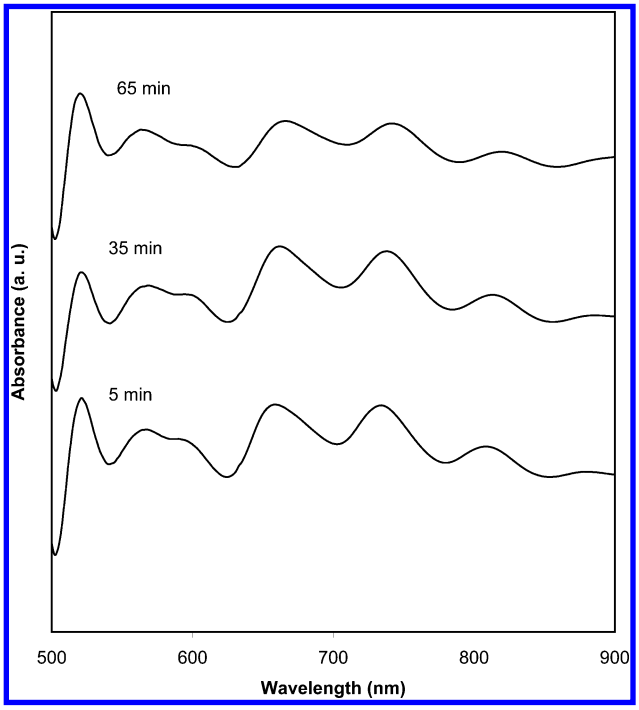

Figure 12. NIR spectra of NaDDBS−SWNT solutions after various sonication times.

[1 − (D/G)] value. The NIR absorption results were in good agreement with the Raman observations (Figure 12). The relative intensities of the peaks remained constant with the sonication time, and no significant energy shifts were observed. These results indicate that no physical modification of the SWNT was produced at least for the first hour of vigorous sonication.

To further evaluate all the parameters involved in the stability of SWNT−NaDDBS suspensions, we also investigated the effect of the concentration of surfactant, and the results are presented in Figure 13. As observed, there is a minimum concentration of surfactant for the solubilization for a fixed concentration of carbon nanotubes. Because the maximum concentration of adsorbed surfactant can be reached at added concentrations of surfactant below the cmc, the solubilization of SWNT does not have to necessarily coincide with the formation of micelles. In this particular example, the optimum feed concentration of NaDDBS is around 2.5 mM. At this

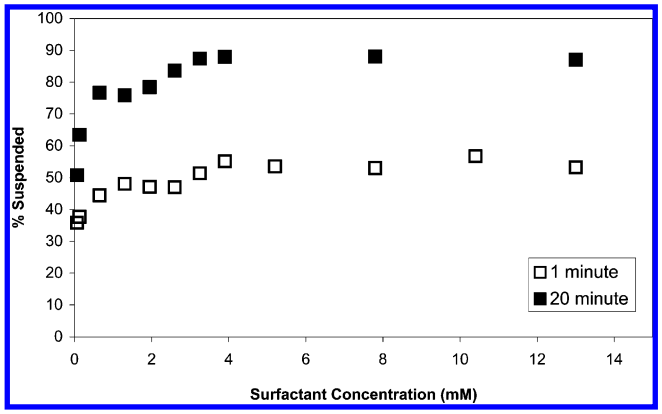

Figure 13. Effect of concentration of NaDDBS on suspendability of SWNT at 1 and 20 min of sonication. The concentration of SWNT is 0.06 mg/mL. Horn dismembrator (600 W, 20 kHz).

concentration the SWNT adsorb surfactant molecules in the bulk, while the free surfactant concentration is reduced; it might even fall below the effective cmc of the system. Above that value, adding extra surfactant means wasting unnecessary material. With these results, we have also demonstrated that it is possible to solubilize a significant amount of SWNT at concentrations of NaDDBS below the cmc. These results demonstrate that micelle formation is not a necessary condition for suspendability of the nanotubes.

4. Conclusions

We have demonstrated that the method employed for the purification of SWNT can have an important effect on surface properties such as the PZC (point of zero charge). Thus, carbon nanotubes can exhibit either negative or positive charges on the surface, depending on the pH of the surrounding media.

Analysis of the adsorption isotherms of the anionic surfactant sodium dodecylbenzenesulfonate (NaDDBS) on SWNT indicates that the interactions between the surfactant molecules and the nanotube walls are mostly hydrophobic in nature. Only at pH values far from the PZC the Coulombic attraction or Coulombic repulsion between the negatively charged headgroups of the surfactant and the charged surface of the nanotubes becomes important. The adsorption studies also revealed that, at saturation, each nanotube is covered by a monolayer of surfactant, in which the molecules rest with the tails oriented vertically on the surface. According to these results, we can conclude that carbon nanotubes are not solubilized in the interior of cylindrical micelles. Instead, adsorbed surfactant is responsible for the effective suspension of the nanotube.

We have also shown that the sonication time plays a key role in the suspendability of SWNT. The surfactant by itself is not capable of suspending the nanotubes effectively without the aid of vigorous sonication.

Finally, from the practical point of view, we have optimized the use of surfactant by determining the minimum needed to suspend a given fraction of nanotubes under different conditions (sonication time, nanotube concentration, etc.). What is important to note is that the minimum amount of surfactant needed to effect the suspension may be below the cmc. Therefore, formation of micelles in solution is not a requirement for suspendability. In fact, once the nanotube surface has been saturated, additional surfactant in solution is not needed and may unnecessarily increase the cost of the process.

Acknowledgment. This research was conducted with financial support from the Department of Energy, Office of Basic Energy Sciences (Grant DE-FG03-02ER15345) and from the University of Oklahoma Bioengineering Center Seed Grant program. The authors also express their gratitude to OCAST for financial support (Grant AR031-004) and the National Science Foundation under Grant EPS-0132534. H.R. acknowledges OCAST for support under the internship program. We are grateful to Prof. N. Hankins for his insightful comments on the manuscript.

References and Notes

(1) Liu, J.; Rinzler, A. G.; Dai, H.; Hafner, J. H.; Bradley, R. K.; Boul, P. J.; Lu, A.; Iverson, T.; Shelimov, K.; Huffman, C. B.; Rodriguez-Macias, F.; Shon, Y. S.; Lee, T. R.; Colbert, D. T.; Smalley, R. E. *Science* **1998**, *280*, 1253.

(2) Zhang, J.; Zou, H.; Qing, Q.; Yang, Y.; Li, Q.; Liu, Z.; Guo, X.; Du, Z. *J. Phys. Chem. B* **2003**, *107* (16), 3712.

(3) Chen, J.; Hamon, M. A.; Hu, H.; Cheng, Y.; Rao, A. M.; Eklund, P. C.; Haddon, R. C. *Science* **1998**, *282*, 95.

(4) Mickelson, E. T.; Chiang, I. W.; Zimmerman, J. L.; Boul, P. J.; Lozano, J.; Liu, J.; Smalley, R. E.; Hauge, R. H.; Margrave, J. L. *J. Phys. Chem. B* **1999**, *103*, 4318.

(5) Boul, P. J.; Liu, J.; Mickelson, E. T.; Huffman, C. B.; Ericson, L. M.; Chiang, I. W.; Smith, K. A.; Colbert, D. T.; Hauge, R. H.; Margrave, J. L.; Smalley, R. E. *Chem. Phys. Lett.* **1999**, *310*, 367.

(6) Bahr, J. L.; Yang, J.; Kosynkin, D. V.; Bronikowski, M. J.; Smalley, R. E.; Tour, J. M. *J. Am. Chem. Soc.* **2001**, *123*, 6536.

(7) Bahr, J. L.; Yang, J.; Kosynkin, D. V.; Bronikowski, M. J.; Smalley, R. E.; Tour, J. M. *J. Am. Chem. Soc.* **2001**, *123*, 6536.

(8) Chen, J.; Rao, A. M.; Lyuksyutov, S.; Itkis, M. E.; Hamon, M. A.; Cohn, R. W.; Eklund, P. C.; Colbert, D. T.; Smalley, R. E.; Haddon, R. C. *J. Phys. Chem. B* **2001**, *105*, 2525.

(9) Riggs, J. E.; Walker, D. B.; Carrl, D. L.; Sun, Y.-P. *J. Phys. Chem. B* **2000**, *104*, 7071.

(10) Pompeo, F.; Resasco, D. E. *Nano Lett.* **2002**, *2* (4), 369.

(11) Georgakilas, V.; Tagmatarchis, N.; Pantarotto, D.; Bianco, A.; Briand, J. P.; Prato, M. *Chem. Commun.* **2002**, *24*, 3050.

(12) Dwyer, C.; Guthold, M.; Falvo, M.; Washburn, S.; Superfine, R.; Erie, D.; *Nanotechnology* **2002**, *13*, 601.

(13) Baker, S. E.; Cai, W.; Lasseter, T. L.; Weidkamp, K. P.; Hamers, R. J. *Nano Lett.* **2002**, *2* (12), 1413.

(14) Garg, A.; Sinnott, S. B. *Chem. Phys. Lett.* **1998**, *295*, 273.

(15) Bahr, J. L.; Yang, J.; Kosynkin, D. V.; Bronikowski, M. J.; Smalley, R. E.; Tour, J. M. *J. Am. Chem. Soc.* **2001**, *123*, 6536.

(16) Barraza, H.; Pompeo, F.; O'Rear, E.; Resasco, D. E. *Nano Lett.* **2002**, *2*, 797.

(17) Islam, M. F.; Rojas, E.; Bergey, D. M.; Johnson, A. T.; Yodh, A. G. *Nano Lett.* **2003**, *3* (2), 269.

(18) Kitiyanan, B.; Alvarez, W. E.; Harwell, J. H.; Resasco, D. E. *Chem. Phys. Lett.* **2000**, *317*, 497.

(19) Herrera, J. E.; Balzano, L.; Borgna, A.; Alvarez, W. E.; Resasco, D. E. *J. Catal.* **2001**, *204*, 129.

(20) Alvarez, W. E.; Pompeo, F.; Herrera, J. E.; Balzano, L.; Resasco, D. E. *Chem. Mater.* **2002**, *14*, 1853.

(21) Herrera, J. E.; Balzano, L.; Pompeo, F.; Resasco, D. E. *J. Nanosci. Nanotechnol.* **2003**, *3*, 133−138.

(22) Hankins, N. P.; O'Haver, J. H.; Harwell, J. H. *Ind. Eng. Chem. Res.* **1996**, *35* (9), 2844.

(23) Zajac, J.; Trompette, J. L.; Partyka, S. *Langmuir* **1996**, *12* (5), 1357.

(24) Goloub, T. P.; Koopal, L. K.; Bijsterbosch, B. H.; Sidorova, M. P. *Langmuir* **1996**, *12* (13), 3188.

(25) Drach, M.; Rudzinski, W.; Narkiewicz-Michalek, J. *J. Dispersion Sci. Technol.* **2000**, *21* (6), 683.

(26) Scamehorn, J. F.; Schechter, R. S.; Wade, W. H. *J. Colloid Interface Sci.* **1982**, *85* (2), 483.

(27) Roberts, B. L.; Scamehorn, J. F.; Harwell, J. H. *ACS Symp. Ser.* **1986**, *311*, 200.

(28) *Solubilization in Surfactant Aggregates*; Christian, S. D., Scamehorn, J. F., Eds.; Marcel Dekker: New York, 1995.

(29) Rosen, M. J. *Surfactants and Interfacial Phenomena*; John Wiley and Sons: New York, 1989.

(30) Adamson, A. W. *Physical Chemistry of Surfaces*; Wiley: New York, 1997.

(31) Sun, J.; Gao, L.; Li, W. *Chem. Mater.* **2002**, *14*, 5169.

(32) Jiang, L.; Gao, L.; Sun, J. *J. Colloid Interface Sci.* **2003**, *260*, 89.

(33) Sano, M.; Okamura, J.; Shinkai, S. *Langmuir* **2001**, *17*, 7172.

(34) Li, Y.-H.; Wang, S.; Luan, Z.; Ding, J.; Xu, C.; Wu, D. *Carbon* **2003**, *41* (5), 1057.

(35) Akratopulu, K. Ch.; Vordonis, L.; Lycourghiotis, A. *J. Catal.* **1988**, *109*, 41.
(36) Korah, J.; Spieker, W. A.; Regalbuto, J. R. *Catal. Lett.* **2003**, *85* (1−2), 123.
(37) Spieker, W. A.; Regalbuto, J. R.; Rende, D.; Bricker, M.; Chen, Q. *Stud. Surf. Sci. Catal.* **2000**, *130*, 203.
(38) Mieth, J. A.; Schwarz, J. A.; Huang, Y.-J.; Fung, S. C. *J. Catal.* **1990**, *122*, 202.
(39) Chen, R. J.; Zhang, Y.; Wang, D.; Dai, H. *J. Am. Chem. Soc.* **2001**, *123*, 3838.
(40) Zettlemoyer, A. C. *J. Colloid Interface Sci.* **1968**, *28*, 343.
(41) Djuve, J.; Grant, L. M.; Sjöblom, J.; Goulob, T. P.; Pugh, R. J. *Langmuir* **2002**, *18*, 2673.
(42) Király, Z.; Findenegg, G. H. *J. Phys. Chem. B* **1998**, *102*, 1203.
(43) Király, Z.; Findenegg, G. H. *Langmuir* **2000**, *16*, 8842.
(44) Király, Z.; Findenegg, G. H.; Klumpp, E.; Shlimper, H.; Dékány, I. *Langmuir* **2001**, *17*, 2420.
(45) Hafner, J. H.; Bronikowski, M. J.; Azamian, B. R.; Nikolaev, P.; Rinzler, A. G.; Colbert, D. T.; Smith, K. A.; Smalley, R. E. *Chem. Phys. Lett.* **1998**, *296*, 195.
(46) Nikolaev, P.; Bronikowski, M. J.; Bradley, R. K.; Rohmund, F.; Colbert, D. T.; Smith, K. A.; Smalley, R. E. **1999**, *313*, 91.
(47) Bronikowski, M. J.; Willis, P. A.; Colbert, D. T.; Smith, K. A.; Smalley, R. E. *J. Vac. Sci. Technol.* **2001**.
(48) O'Connell, M. J.; Bachilo, S. M.; Huffman, C. B.; Moore, V. C.; Strano, M. S.; Haroz, E. H.; Rialon, K. L.; Boul, P. J.; Noon, W. H.; Kittrell, C.; Ma, J.; Hauge, R. H.; Weisman, R. B.; Smalley, R. E. *Science* **2002**, *297*, 593.
(49) Strano, M. S.; Moore, V. C.; Miller, M. K.; Allen, M. J.; Haroz, E. H.; Kittrell, C.; Hauge, R. H.; Smalley, R. E. *J. Nanosci. Nanotechnol.* **2003**, *3* (1−2), 81.
(50) Zhou, W.; Ooi, Y. H.; Russo, R.; Papanek, P.; Luzzi, D. E.; Fischer, J. E.; Bronikowski, M. J.; Willis, P. A.; Smalley, R. E. *Chem. Phys. Lett.* **2001**, *350*, 6.
(51) Liu, J. F.; Ducker, W. A. *J. Phys. Chem. B* **1999**, *103*, 8558.
(52) Bachilo, S. M.; Balzano, L.; Herrera, J. E.; Pompeo, F.; Resasco, D. E.; Weisman, R. B. *J. Am. Chem. Soc.* **2003**, *125*, 11186.
(53) Cinke, M.; Li, J.; Chen, B.; Cassell, A.; Delzeit, L.; Han, J.; Meyyappan, M.; *Chem. Phys. Lett.* **2002**, *365*, 69.
(54) Scamehorn, J. F.; Schechter, R. S.; Wade, W. H. *J. Colloid Interface Sci.* **1982**, *85*, 463.
(55) Wu, J.; Harwell, J. H.; O'Rear, E. *Langmuir* **1987**, *3*, 531.
(56) Khan, M. G. C.; Banerjee, S.; Wong, S. S. *Nano Lett.* **2002**, *2* (11), 1215.
(57) Hilding, J.; Grulke, E. A.; Zhang, Z. G.; Loockwood, F. *J. Dispersion Sci. Technol.* **2003**, *24* (1), 1.
(58) Huang, W.; Lin, Y.; Taylor, S.; Gaillard, J.; Rao, A. M.; Sun, Y.-P. *Nano Lett.* **2002**, *2* (3), 231.
(59) Nakashima, N.; Tomonari, Y.; Murakami, H. *Chem. Lett.* **2002**, 638.
(60) Park, C.; Ounaies, Z.; Watson, K. A.; Crooks, R. E.; Smith, J.; Lowther, S. E.; Connell, J. W.; Siochi, E. J.; Harrison, J. S.; St. Clair, T. L. *Chem. Phys. Lett.* **2002**, *364* (3−4), 303.
(61) Mukhopadhyay, K.; Dwivedi, C. D.; Mathur, G. N. *Carbon* **2002**, *40*, 1373.
(62) Jeong, S.-H.; Lee, O.-J.; Lee, K.-H. *Chem. Mater.* **2002**, *14*, 1859.